molecular pharmaceutics

articles

Intracellular Processing of Riboflavin in Human Breast Cancer Cells

Lisa M. Bareford,[†] Mitch A. Phelps,[‡] Amy B. Foraker,[†,§] and Peter W. Swaan*[,†]

Department of Pharmaceutical Sciences, Center for Nanomedicine and Cellular Delivery, University of Maryland, Baltimore, Maryland 21201, and Biophysics Program and Division of Pharmaceutics, The Ohio State University, Columbus, Ohio 43210

Received April 21, 2008; Revised Manuscript Received August 11, 2008; Accepted August 19, 2008

Abstract: A variety of polarized epithelial cells, such as human breast cancer (MCF-7), have mechanistically evolved the ability to adapt to the dynamic cellular environment and maintain homeostasis of an array of micronutrients which display conditional requirements. Active absorption mechanisms, including endocytosis, are able to control cell surface recognition and protein expression which are associated with a substance's intracellular processing and kinetics. Riboflavin (RF), or vitamin B2, has been recognized as an important factor in a multitude of terminal disease states, most notably in breast cancer, where its cellular absorption is significantly enhanced. In order to delineate the regulatory mechanisms and kinetics associated with RF control in human breast cancer tissue, this study aimed to model its absorption profile and identify its intracellular regulatory components. Using both the Michaelis−Menten equation and a modified version of it, incorporating both active internalization and passive diffusion, RF absorption displayed better correlation ($r^2 >$ 0.998) with the mixed, active and passive, model exhibiting kinetic parameters characteristic of a receptor-mediated uptake mechanism ($J_{max} = 2.58$ pmol/5 min, $K_m = 106$ nM) at extracellular RF concentrations under 5 μM and a passive component existing at RF concentrations greater than 5 μM. Following internalization, RF was able to recycle back to the membrane with a half-life of 13.7 min at 37 °C, which occurred more rapidly with increasing extracellular RF concentrations ($t_{1/2} =$ 5.4 min at 1 μM) and decreasing temperatures ($t_{1/2} = 6.4$ min at 4 °C). Furthermore, modification to endosomal pH using the lysomotropic agents monensin (25 μM) and primaquine (300 μM) significantly inhibited the exocytosis of RF (61 and 30% of control), whereas biochemical modification of endocytic trafficking with okadaic acid (1 μM) led to a significant increase in RF exocytosis (208%). In conclusion, RF homeostasis in MCF-7 cells is a well regulated process which is dependent upon RF concentration, temperature, and endosomal acidification.

Keywords: Riboflavin; endocytosis; exocytosis; intracellular kinetics; MCF-7 cells

Introduction

Riboflavin (RF), a water soluble vitamin (B2), is necessary for cellular growth and development through the mitochondrial utilization of its cofactors flavin mononucleotide (FMN) and flavin adenine dinucleotide (FAD).[1] Whereas FMN and FAD are essential in catalyzing oxidation/reduction reactions in the mitochondrial electron transport chain of all eukaryotic cells, RF remains the only absorptive species of flavin. Mammals are unable to synthesize RF; therefore, it must be acquired from the diet to prevent clinical manifestations of RF deficiency, which includes growth retardation and neurodegenerative disorders.[2] Interestingly, RF has been ascribed a role in breast cancer progression, as evidenced by a

* To whom correspondence should be addressed. Department of Pharmaceutical Sciences, University of Maryland, 20 Penn Street, Health Sciences Facility 2, Baltimore, MD 21201. Telephone: (410) 706-0103. Fax: (410) 706-5017. E-mail: pswaan@rx.umaryland.edu.

† University of Maryland.

‡ The Ohio State University.

§ Current address: Departments of Biopharmaceutical Sciences and Pharmaceutical Chemistry, University of California, San Francisco, CA 94143.

(1) Foraker, A. B.; Khantwal, C. M.; Swaan, P. W. Current perspectives on the cellular uptake and trafficking of riboflavin. *Adv. Drug. Deliv. Rev.* **2003**, *55*, 1467–1483.

10.1021/mp800046m CCC: $40.75
Published on Web 08/29/2008

significant decrease in RF serum levels[3] and elevation of its plasma carrier protein.[4]

Maintaining the cellular homeostasis of micronutrients, such as RF, is a dynamic and controlled process. Putative protein(s) responsible for the cellular uptake pathway have been identified only very recently, and preliminary data suggest the involvement of a possible G-protein coupled receptor/transporter protein ($K_m \sim 30-60$ nM).[5] In line with these recent developments, previous studies in our laboratory demonstrated that RF absorption occurs through a receptor-mediated endocytic (RME) mechanism which is temperature-, energy-, and concentration-dependent.[6−10] Following vesicular internalization, endosomes containing RF traffic along cytoskeletal scaffolds[9] to associate with subcellular endocytic compartments, namely, early endosomes and lysosomes, as well as the golgi and mitochondria to a lesser extent.[9] A variety of other high affinity RME ligands, including transferrin,[11] ricin,[12] apolipoprotein E,[13] and insulin,[14] follow a similar internalization mechanism resulting in tightly regulated intracellular processing pathways. Depending on the vesicular cargo, endosomes may follow a maturation pathway involving early endosomes, sorting endosomes, and late endosomes while associating and interacting with several subcellular compartments including golgi, mitochondria, and lysosomes.[15] The majority of receptors, and a fraction of internalized ligand, follow a default recycling pathway back to the plasma membrane where the receptors may sequester additional ligand.[16]

Although the fate of RME ligands is tightly controlled, their intracellular pathway can be affected by biochemical stimuli or disease states and may result in disrupted intracellular trafficking, potential missorting to alternative cellular compartments, and/or release of intact ligand from the cell. For example, the subcellular trafficking of epidermal growth factor (EGF) was found to be significantly altered in prostate cancer cells (PC3),[17] emphasizing the implications of disease-associated cellular regulation. Given the critical role of RF in various pathological conditions, the physiological and biochemical components that regulate intracellular processing of RF require further definition.

The present study aims to delineate the physiological and biochemical parameters controlling the rate and extent of RF internalization and subcellular processing in order to construct a comprehensive cellular pharmacokinetic model for this important vitamin. This was accomplished by integrating data from previous studies and recording the subcellular fate of RF with regard to ligand concentration, temperature, endosomal pH, and cytoskeletal trafficking. Mathematical models are developed to describe the affinity and capacity of cell surface uptake mechanisms comprising both active as well as passive absorption components. We have previously demonstrated the predominance of a passive component in oversupplemented conditions,[18] that is, at RF concentrations above normal human plasma levels (>12 nM), and an active component via high affinity receptors below or near basal RF concentrations (~12 nM).[6] In addition, confocal analysis of fluorescently labeled RF has provided

(2) Said, H. M.; Ma, T. Y. Mechanism of riboflavine uptake by Caco-2 human intestinal epithelial cells. *Am. J. Physiol.* **1994**, *266*, G15–G21.
(3) Vaidya, S. M.; Kamlakar, P. L.; Kamble, S. M. Molybdenum, xanthine oxidase and riboflavin levels in tamoxifen treated postmenopausal women with breast cancer. *Indian J. Med. Sci.* **1998**, *52*, 244–247.
(4) Rao, P. N.; Levine, E.; Myers, M. O.; Prakash, V.; Watson, J.; Stolier, A.; Kopicko, J. J.; Kissinger, P.; Raj, S. G.; Raj, M. H. Elevation of serum riboflavin carrier protein in breast cancer. *Cancer Epidemiol., Biomarkers Prev.* **1999**, *8*, 985–990.
(5) Yonezawa, A.; Masuda, S.; Katsura, T.; Inui, K. I. Identification and functional characterization of a novel human and rat riboflavin transporter, RFT1. *Am. J. Physiol. Cell Physiol.*, published online July 16, http://dx.doi.org/10.1152/ajpcell.00019.2008.
(6) Huang, S. N.; Swaan, P. W. Involvement of a receptor-mediated component in cellular translocation of riboflavin. *J. Pharmacol. Exp. Ther.* **2000**, *294*, 117–125.
(7) Huang, S. N.; Swaan, P. W. Riboflavin uptake in human trophoblast-derived BeWo cell monolayers: cellular translocation and regulatory mechanisms. *J. Pharmacol. Exp. Ther.* **2001**, *298*, 264–271.
(8) Huang, S. N.; Phelps, M. A.; Swaan, P. W. Involvement of endocytic organelles in the subcellular trafficking and localization of riboflavin. *J. Pharmacol. Exp. Ther.* **2003**, *306*, 681–687.
(9) D'Souza, V. M.; Foraker, A. B.; Free, R. B.; Ray, A.; Shapiro, P. S.; Swaan, P. W. cAMP-Coupled Riboflavin Trafficking in Placental Trophoblasts: A Dynamic and Ordered Process. *Biochemistry* **2006**, *45*, 6095–6104.
(10) Mason, C. W.; D'Souza, V. M.; Bareford, L. M.; Phelps, M. A.; Ray, A.; Swaan, P. W. Recognition, co-internalization, and recycling of an avian riboflavin carrier protein in human placental trophoblasts. *J. Pharmacol. Exp. Ther.* **2006**, *317*, 465–472.
(11) Dautry-Varsat, A.; Ciechanover, A.; Lodish, H. F. pH and the recycling of transferrin during receptor-mediated endocytosis. *Proc. Natl. Acad. Sci. U.S.A.* **1983**, *80*, 2258–2262.
(12) Magnusson, S.; Kjeken, R.; Berg, T. Characterization of two distinct pathways of endocytosis of ricin by rat liver endothelial cells. *Exp. Cell Res.* **1993**, *205*, 118–125.
(13) Rensen, P. C.; Jong, M. C.; van Vark, L. C.; van der Boom, H.; Hendriks, W. L.; van Berkel, T. J.; Biessen, E. A.; Havekes, L. M. Apolipoprotein E is resistant to intracellular degradation in vitro and in vivo. Evidence for retroendocytosis. *J. Biol. Chem.* **2000**, *275*, 8564–8571.
(14) Dahl, D. C.; Tsao, T.; Duckworth, W. C.; Mahoney, M. J.; Rabkin, R. Retroendocytosis of insulin in a cultured kidney epithelial cell line. *Am. J. Physiol.* **1989**, *257*, C190–C196.
(15) Mukherjee, S.; Ghosh, R. N.; Maxfield, F. R. Endocytosis. *Physiol. Rev.* **1997**, *77*, 759–803.
(16) Linderman, J. J.; Lauffenburger, D. A. Analysis of intracellular receptor/ligand sorting. Calculation of mean surface and bulk diffusion times within a sphere. *Biophys. J.* **1986**, *50*, 295–305.
(17) Bonaccorsi, L.; Nosi, D.; Muratori, M.; Formigli, L.; Forti, G.; Baldi, E. Altered endocytosis of epidermal growth factor receptor in androgen receptor positive prostate cancer cell lines. *J. Mol. Endocrinol.* **2007**, *38*, 51–66.
(18) Foraker, A. B.; Walczak, R. J.; Cohen, M. H.; Boiarski, T. A.; Grove, C. F.; Swaan, P. W. Microfabricated porous silicon particles enhance paracellular delivery of insulin across intestinal Caco-2 cell monolayers. *Pharm. Res.* **2003**, *20*, 110–116.

a blueprint for RF intracellular localizations,[19] illustrating its time-dependent colocalization with early endosomes and lysosomes and to a lesser extent with golgi and mitochondria compartments.[9] Here, we follow RF internalization in response to environmental stimuli and biochemical modifiers to specifically elucidate the importance of an array of intracellular events, such as ligand−receptor dissociation, compartmental sorting,[15] degradation, and recycling.[20] The resulting aggregate kinetic description of RF uptake and trafficking was visualized using a comprehensive model that delineates the dynamic interplay of vesicular processes. This model may be used subsequently to optimize drug delivery schemes using RF as a chemotherapeutic targeting moiety.

Experimental Section

Materials. [^{3}H]-Riboflavin (25 Ci/mmol) and monensin sodium were purchased from Sigma (St. Louis, MO). Okadaic acid was purchased from EMD Biosciences (San Diego, CA). [^{3}H]-Folic acid (25 Ci/mmol) was purchased from American Radiolabeled Chemicals (St. Louis, MO). Primaquine phosphate was purchased from LKT Laboratories, Inc. (St. Paul, MN).

Cell Culture. MCF-7 and SKBR-3 cells were obtained from American Type Culture Collection (Manasas, VA) and maintained at 37 °C under 5% CO_2.

For studies focused on kinetic modeling of both passive and active RF internalization, MCF-7 and SKBR-3 cells were grown in custom-prepared Minimum Essential Medium (MEM) containing ∼266 nM RF or without RF. Media were produced in the laboratory following the MEM formulation (Invitrogen, Carlsbad, CA) with all components added except RF. The media were supplemented with 10% charcoal-stripped fetal bovine serum (FBS; Hyclone, Logan, UT), 1% nonessential amino acids, 100 U/mL penicillin, and 100 ug/mL streptomycin. Charcoal-stripped FBS contains approximately 6.65 nM RF, thereby supplementing a negligible amount (<2.5%) of RF to complete media. These media were then split in two. One half received a 100× riboflavin solution in water to achieve a RF final concentration of ∼266 nM (MEM). The other half received an equal amount of water (RF-free MEM). Media were sterilized through 0.22 μm filters. For recycling studies, all cells were cultured in RF replete media.

RF Uptake. Transport kinetic parameters were determined by measuring initial uptake velocities in SKBR-3 and MCF-7 cells grown in RF deplete media. For accurate determinations, one must ensure that steady-state velocities are being measured as opposed to velocities observed after uptake begins to saturate due to accumulation of substrate in the intracellular compartment. Preliminary studies in COS-1 cells exhibited a linear fit to all data points ($R^2 = 0.998$), implying that steady state was maintained throughout the range of times included (not shown); therefore, 5 min was chosen as an efficient RF incubation time for both cell lines. Cells were seeded in 24-well plates until 80−90% confluence (24−48 h); cells were washed with phosphate-buffered saline (PBS), pH 7.4 and incubated for 5 min at 37 °C in bathing media (BM, HBSS with 25 mM glucose and 10 mM HEPES, pH 7.4) containing 0−40 μM riboflavin and 5 nM [^{3}H]-riboflavin with a specific activity of 41 Ci/mmol. Uptake media were removed, cells were washed three times with 4 °C PBS (pH 7.4), and then cells were lysed with 1 M NaOH for 2 h at 37 °C. Lysates were neutralized with HCl, and the amount of radioactivity in cell lysates was quantified using a Beckman liquid scintillation counter (model LS 6000IC). The protein concentration in cell lysates was determined with the Bio-Rad protein assay.

Ligand Recycling and Inhibition Studies. Transferrin (TF) was labeled with Na-^{125}I (∼5 μCi/μg; Amersham Biosciences, Piscataway, NJ) according to established methods using the IODOGEN technique (Pierce Biotechnology, Inc., Rockford, IL). The specific activity of ^{125}I-TF was 400 cpm/pmol.

Prior to recycling studies, experiments were conducted to measure the amount of RF, as well as control ligands TF and folic acid (FA), that passively diffused out of cells under the experimental conditions to be used for recycling assays. Here, MCF-7 cells were preloaded with 10 nM [^{3}H]-RF, for 20 min at 37 °C followed by removal of all nonspecific and uninternalized ligand. Cells were then placed at 4 °C, in order to prevent active transport, and incubated in prechilled media for up to 1 h followed by radioactive quantification of extracellular RF. Results indicated that 40 pM RF was passively released from MCF-7 cells under these experimental conditions. This amount of unlabeled RF was supplemented in the media used for RF recycling studies, thereby equilibrating intracellular and extracellular ligand[21] in order to accurately measure its active efflux via exocytosis. Similar experiments were conducted to determine the amount of passively diffusing [^{3}H]-FA and ^{125}I-TF.

Cells were seeded in Costar 24-well plates (Fisher Scientific, Pittsburgh, PA) at a density of 5×10^4 cells/cm^2 and used 4 days later in ligand uptake and recycling studies. For temperature-dependence studies, cells were incubated for 20 min with 10 nM [^{3}H]-RF, 10 nM [^{3}H]-FA (caveolae-mediated RME ligand), or 10 nM ^{125}I-TF (clathrin-dependent RME ligand) at 37 °C, followed by removal of all nonspecific binding ligand via three quick, neutral DPBS washes and collection of membrane-associated ligand using a 10 min acidic, ice-cold DPBS (pH 3.0) wash. Recycling (i.e., exocytosis) was then allowed for up to 1 h at 4, 16, or 37

(19) Phelps, M. A.; Foraker, A. B.; Gao, W.; Dalton, J. T.; Swaan, P. W. A Novel Rhodamine-Riboflavin Conjugate Probe Exhibits Distinct Fluorescence Resonance Energy Transfer That Enables Riboflavin Trafficking and Subcellular Localization Studies. *Mol. Pharmaceutics* **2004**, *1*, 257–266.

(20) Maalmi, M.; Strieder, W.; Varma, A. Ligand diffusion and receptor mediated internalization: Michaelis-Menten kinetics. *Chem. Eng. Sci.* **2001**, *56*, 5609–5616.

(21) Harford, J.; Wolkoff, A. W.; Ashwell, G.; Klausner, R. D. Monensin inhibits intracellular dissociation of asialoglycoproteins from their receptor. *J. Cell Biol.* **1983**, *96*, 1824–1828.

°C, where recycling media was supplemented with an experimentally determined amount of passively diffusing ligand (see above). For concentration-dependent studies, cells were supplied with media containing 0.005−1 μM unlabeled ligand and incubated at 37 °C for recycling. The effects of altering endosomal pH and microtubular trafficking on ligand recycling were evaluated using lysomotropic agents monensin (2.5−25 μM), primaquine (100−300 μM), and okadaic acid (0.1−1 μM). Cells were pretreated for 30 min with monensin, primaquine, or okadaic acid and then dosed with either 10 nM [^{3}H]-RF, 10 nM [^{3}H]-FA, or 10 nM ^{125}I-TF for 20 min at 37 °C in the continued presence or absence of modifying agents, followed by recycling at 37 °C.

For all recycling treatments, samples (500 μL) were collected from the media at 1, 5, 15, 30, 45, and 60 min and then replenished with equivalent volumes of prewarmed fresh media containing unlabeled ligand in order to maintain consistent volumes and sink conditions. Extracellular amounts of exocytosed ligand as well as any remaining intracellular ligand, following cell lysis, were measured by liquid scintillation counting for tritiated samples and gamma counting for iodinated samples. Data were normalized to total protein content, as ligand transport was limited to membrane receptor based mechanisms, and expressed as a percentage of untreated control for each variable. Viability was tested using the CellTiter Nonradioactive Cell Proliferation Assay (Promega, Madison, WI) with ≥90% viability versus untreated cells considered acceptable as the threshold value. Results were expressed as percent total amount recycled of amount dosed. The recycling half-life ($t_{1/2}$) was determined using first-order kinetics (Prism 4.0, Graph Pad Software Inc., San Diego, CA) according to the equation

$$t_{1/2} = 0.693/k \tag{1}$$

where k is the recycling rate constant.

Statistics. Results were expressed as mean ± standard deviation (SD). Statistical analyses between groups in the kinetic uptake studies were performed using a Student's *t*-test and one-way analysis of variance (ANOVA) for single and multiple comparisons. Each variable in the recycling studies was analyzed using one-way ANOVA followed by intergroup comparison using the Newman−Keuls multiple comparison test. Significant differences were reported with a confidence interval of 95%.

Kinetic Analysis of RF Binding and Early Endosomal Trafficking. MCF-7 cells were cultured and seeded as previously described. A homologous competitive experiment was used to determine the affinity of RF to its membrane bound receptor. Here, cells were pulsed with 10 nM [^{3}H]-RF for 5 min at 4 °C, followed by the removal of all nonspecific ligand using four DPBS pH 7.4 washes. Cells were then incubated in increasing concentrations of cold RF (0−1000 nM) for 5 min at 4 °C. The remaining membrane bound fraction of [^{3}H]-RF was collected using an acidic wash with DPBS pH 3 for 10 min. Bound fractions were counted in a liquid scintillation counter, and RF binding affinity (k_d) was determined using a nonlinear regression analysis for one-site binding (Graphpad Prism, v. 4). In order to measure the dissociation rate of RF from its cell surface receptor, MCF-7 cells were pulsed with [^{3}H]-RF for 5 min and washed with DPBS pH 7.4 to remove all nonspecifically bound ligand. [^{3}H]-RF was then displaced using 100 nM cold RF for 0−60 min. The remaining membrane bound fraction was collected and counted as described. The dissociation rate constant (k_{off}) was determined using a nonlinear regression analysis for one phase exponential decay (Graphpad Prism, v. 4). Using recycling half-lives, the rate of RF trafficking between early endosomal compartments was determined using eq 1.

Results

RF Uptake Kinetics. Previous reports for RF transport have employed either a standard Michaelis−Menten model (eq 2)[22] or a mixed model containing a saturable component along with a linear passive component (eq 3).[7] The mixed model was developed to provide a more accurate kinetic interpretation for molecules possessing both passive and active translocation components by measuring each mechanism separately.[23] Kinetic uptake parameters, such as the concentration at half-maximal transport rate (K_t, Michaelis−Menten-type constant), the maximal uptake rate (J_{max}), and the passive membrane permeability coefficient (P_m), were calculated using WinNonlin (Pharsight, Mountain View, CA) by weighted nonlinear least-squares regression analysis of experimental results to the following expressions:

$$J = \frac{J_{max}C}{K_t + C} \tag{2}$$

$$J = \frac{J_{max}C}{K_t + C} + P_m C \tag{3}$$

where J represents the total flux and C is the RF concentration.

Figure 1 illustrates both models when employed to experimental data generated in MCF-7 cells, similar to the resulting profile for SKBR-3 cells. Residual plots are included to show the differences in prediction accuracy between the two models and illustrate that a mixed model provides lower residual values distributed more evenly about the predicted values (Figure 1D). In addition, χ^2 and diagnostic parameter values calculated in WinNonlin indicated an improved fit when the passive component was included (data not shown). Thus, the mixed model provides a better fit compared to the Michaelis−Menten model alone. The data were analyzed separately for both the saturable and passive components. In the MCF-7 cells, RF resulted in a J_{max} value of 2.58 pmol/mg protein/5 min, with an affinity

(22) Said, H. M.; Ortiz, A.; Ma, T. Y.; McCloud, E. Riboflavin uptake by the human-derived liver cells Hep G2: mechanism and regulation. *J. Cell Physiol.* **1998**, *176*, 588–594.

(23) Acharya, P.; O'Connor, M. P.; Polli, J. W.; Ayrton, A.; Ellens, H.; Bentz, J. Kinetic identification of membrane transporters that assist P-glycoprotein-mediated transport of digoxin and loperamide through a confluent monolayer of MDCKII-hMDR1 cells. *Drug Metab. Dispos.* **2008**, *36*, 452–460.

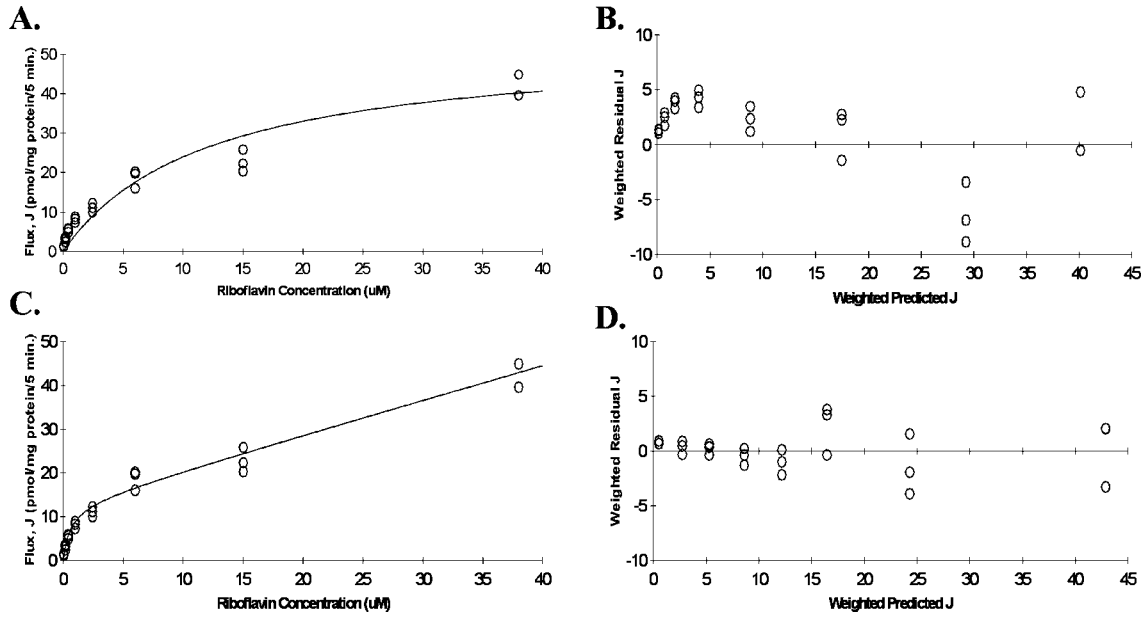

Figure 1. Nonlinear least-squares fits of [^{3}H]-RF uptake data generated in MCF-7 cell cultures. Fits correspond to the use of only a saturable Michaelis−Menten (eq 2) component (A) or both a saturable and passive (eq 3) component (C). Residual plots for fits with Michaelis−Menten only (B) and with the passive component included (D) are also shown.

constant (K_m) equal to 106 ± 9 nM. The passive permeability (P_m) was calculated to be 0.36 μL/mg protein/5 min.

RF Exocytosis in the Presence of Increasing Extracellular RF Concentration. The effect of extracellular RF concentration on apical recycling of RF was determined using a "low cis" experiment.[24] Here, a low concentration of ligand is pulsed into cells, upon which the rate and extent of extracellular ligand release is monitored against increasing extracellular ligand concentrations. These experiments will reveal active externalization of ligand specifically via exocytosis, which can occur against a concentration gradient; this is a unique feature of endocytosed ligand and is not observed for other active or passive transport mechanisms. MCF-7 cells were pulsed with 5 nM [^{3}H]-RF followed by recycling for 1 h against increasing extracellular ligand[21] (0−1000 nM). The amount of RF released (64.2−69.4 pM) remained relatively constant, whereas recycling rates increased ($t_{1/2}$ = 12.5−5.4 min) with increasing RF concentration (Table 1). These results suggest the presence of an active recycling mechanism for RF which would allow for substrate exchange against a concentration gradient.

Temperature Effect on RF Retrograde Transport. At physiological temperatures (37 °C), active transport mechanisms are expected to function optimally, whereas, at reduced temperatures, the ligand may be unable to proceed to the lysosomes for degradation, leading to dissipation and accumulation into the cellular cytosol[25] (<20 °C), or endocytosed ligand may traffic rapidly back to the cell surface to be released extracellularly or reinternalized (4 °C). Retrograde transport of numerous endocytosed ligands has been shown to be significantly reduced at lowered temperature,[26,27] suggesting that apical recycling mechanisms are temperature-dependent. Here, fully differentiated MCF-7 cells were dosed with RF, FA, and TF, followed by the analysis of their extracellular accumulation at 4, 16, and 37 °C. When cells were incubated at 4 °C, only minimal amounts of the recycling ligands RF (23.29 ± 0.05 pM) and TF (14.42 ± 0.19 pM) were released from the cells (Figure 2a). A temperature-dependent decrease in ligand exocytosis was observed at 16 °C for RF (31.99 ± 1.81 pM) and TF (7.72 ± 0.07 pM) (Figure 2b), compared to RF (98.85 ±

Table 1. The Rate of Retroendocytosis for Riboflavin (RF) Increased in the Presence of Extracellular Unlabeled RF, While the Extent of Recycling Remained Constant

extracellular RF (nM)	RF effluxed (pM)	$t_{1/2}$ (min)
0	67.3 ± 5.2	12.5 ± 2.4
5	69.4 ± 7.8	10.9 ± 2.9
20	64.2 ± 8.9	10.8 ± 3.5
100	69.7 ± 8.8	9.9 ± 2.9
500	56.1 ± 9.3	7.3 ± 2.7
1000	64.5 ± 6.8	5.4 ± 1.6

(24) Stein, W. D., Ed. *Channels, Carriers, and Pumps: An Introduction to Membrane Transport*; Academic Press: New York, 1990.
(25) Stefaner, I.; Klapper, H.; Sztul, E.; Fuchs, R. Free-flow electrophoretic analysis of endosome subpopulations of rat hepatocytes. *Electrophoresis* **1997**, *18*, 2516–2522.
(26) Ellinger, I.; Rothe, A.; Grill, M.; Fuchs, R. Apical to basolateral transcytosis and apical recycling of immunoglobulin G in trophoblast-derived BeWo cells: effects of low temperature, nocodazole, and cytochalasin D. *Exp. Cell Res.* **2001**, *269*, 322–331.
(27) Apodaca, G.; Enrich, C.; Mostov, K. E. The calmodulin antagonist, W-13, alters transcytosis, recycling, and the morphology of the endocytic pathway in Madin-Darby canine kidney cells. *J. Biol. Chem.* **1994**, *269*, 19005–19013.

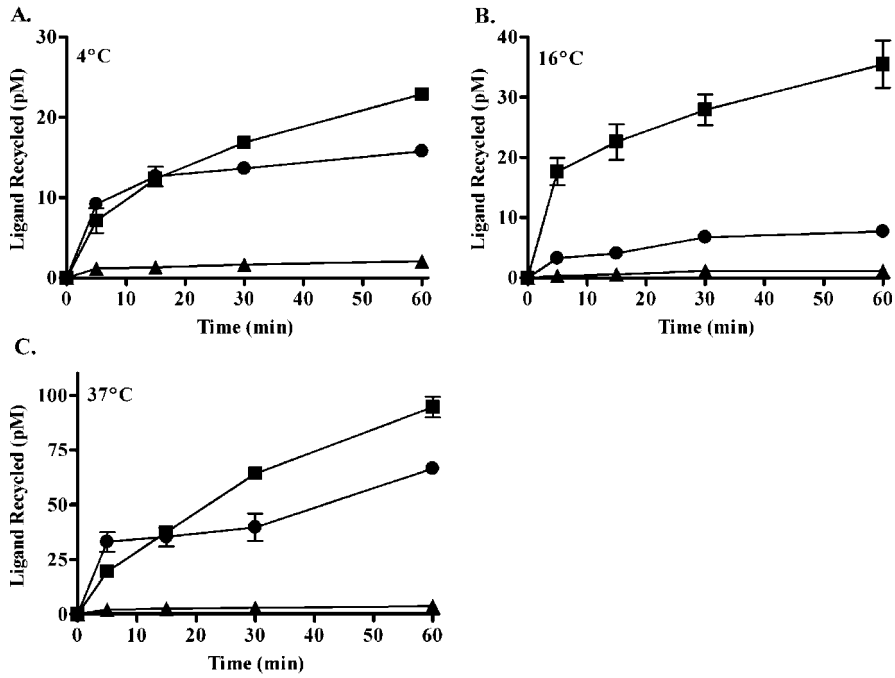

Figure 2. RF exocytosis is temperature-dependent. MCF-7 cells were incubated with 10 nM [^{3}H]-RF for 20 min at 37 °C. The samples were collected for various time points from cells kept at 4, 16, or 37 °C. Extracellular accumulation of [^{3}H]-riboflavin (square), [^{3}H]-folic acid (triangle), and ^{125}I-TF (circle) were determined, and data are expressed as amount of ligand recycled (pM) and represent the mean ± SD of at least six determinations.

Table 2. Lower Temperatures Substantially Reduce Ligand Recycling Half-Lives for Riboflavin (RF) and Transferrin (TF) but Not for Folic Acid (FA)

	$t_{1/2}$ (min)		
T (°C)	RF	TF	FA
4	6.4 ± 2.4	3.7 ± 1.0	4.5 ± 1.9
16	9.4 ± 2.1	10.5 ± 3.8	2.4 ± 0.6
37	13.7 ± 3.5	19.4 ± 9.5	4.5 ± 1.9

0.92 pM) and TF (63.12 ± 0.48 pM) at 37 °C (Figure 2c), whereas FA showed negligible extracellular accumulation at both physiological and reduced temperatures (Figure 2). Recycling profiles revealed first-order kinetics at all temperatures where an increase in temperature allowed for a decrease in the rate of RF and TF exocytosis (Table 2). These data suggest that the recycling of RF and TF is an active, temperature-dependent process in MCF-7 cells. The prevention of both active efflux (exocytic release) and lysosomal association, through lowered temperatures, resulted in a significant reduction in RF and TF retrograde transport in MCF-7 cells.

Effect of Neutralizing Vesicular pH. Monensin, a Na^+ ionophore, allows for the membrane exchange of H^+ for Na^+ ions resulting in an increased pH or neutralization of acidic intracellular compartments including some endosomes, golgi, and lysosomes.[28] Monensin treatment has been shown to interfere with acidic cellular processes such as ligand and receptor dissociation as well as endosomal trafficking.[21] MCF-7 cells were pretreated with 2.5−25 μM monensin for 30 min. The cells were then dosed with 10 nM [^{3}H]-RF, [^{3}H]-FA, or ^{125}I-TF for 1 h in the absence or continued presence of this lysomotropic agent. A dose-dependent decrease in extracellular ligand release was observed for RF and TF (Figure 3a,c). In contrast, the already minimal amount of FA recovered from the extracellular environment remained unaffected (Figure 3b). Monensin incubation resulted in a concentration-dependent decrease in RF and TF extracellular release, thereby effectively limiting the amount of ligand susceptible to continuous internalization (data not shown). These data suggest that endosomal acidification plays an important role in regulating RF and TF recycling mechanisms in MCF-7 cells.

Primaquine, a weak base, internalizes into cells, and it will protonate in acidic cellular organelles, thereby neutralizing these compartments.[29] This lysomotropic agent also causes osmotic swelling of the trans-Golgi and consequently interferes with the retrograde trafficking of vesicles to the plasma membrane.[30] MCF-7 cells were incubated with 100−300 μM primaquine for 30 min prior to dosing with

(28) Mollenhauer, H. H.; Morre, D. J.; Rowe, L. D. Alteration of intracellular traffic by monensin; mechanism, specificity and relationship to toxicity. *Biochim. Biophys. Acta* **1990**, *1031*, 225–246.

(29) Schwartz, A. L.; Strous, G. J.; Slot, J. W.; Geuze, H. J. Immunoelectron microscopic localization of acidic intracellular compartments in hepatoma cells. *EMBO J.* **1985**, *4*, 899–904.

(30) van Weert, A. W.; Geuze, H. J.; Groothuis, B.; Stoorvogel, W. Primaquine interferes with membrane recycling from endosomes to the plasma membrane through a direct interaction with endosomes which does not involve neutralisation of endosomal pH nor osmotic swelling of endosomes. *Eur. J. Cell Biol.* **2000**, *79*, 394–399.

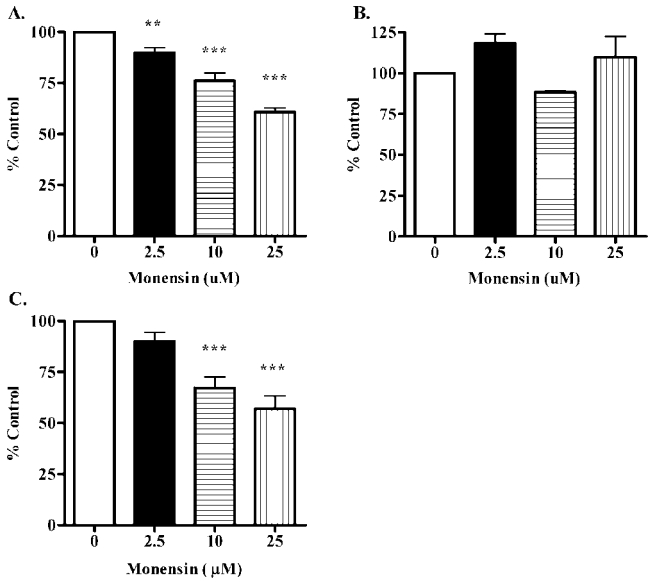

Figure 3. Monensin alters ligand recycling of RF and TF. Cells were preincubated with or without monensin for 30 min, followed by a 20 min coincubation period with [^{3}H]-RF, ^{125}I-TF, or [^{3}H]-FA to allow for ligand recycling at 37 °C. Recycled amounts of [^{3}H]-RF (a), ^{125}I-TF (b), and [^{3}H]-FA (c) after 2.5 μM (solid black bar), 10 μM (horizontal striped bar), 25 μM (vertical striped bar), and no (open bar) treatment were determined by liquid scintillation and gamma counting and were normalized to total protein content. Control cells were treated with buffer alone. Results were expressed as a percentage of recycled ligand detected for untreated cells. These data are expressed as a percentage of control and represent the mean ± SD of at least six determinations. Statistical significance between monensin-treated and untreated cell populations was defined by one-way ANOVA with the Newman−Keuls multiple comparison test (**, $p \leq 0.01$; ***, $p \leq 0.001$).

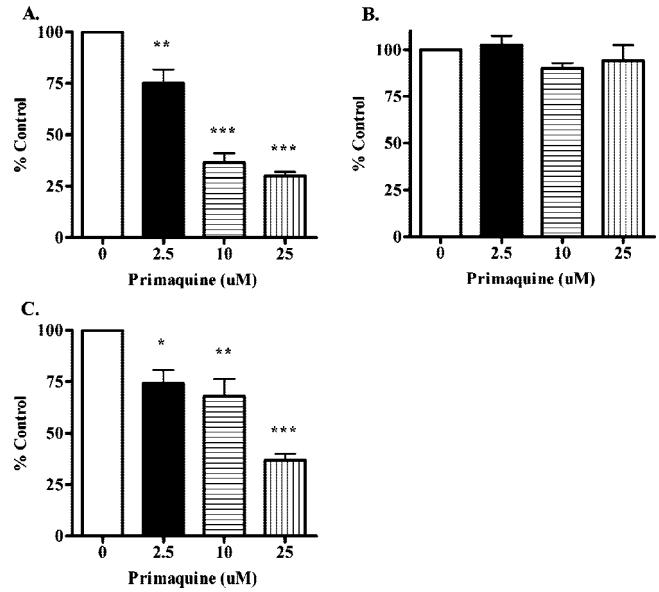

Figure 4. Primaquine decreases cellular release of RF and TF. MCF-7 cells were preincubated with or without primaquine for 30 min, followed by a 20 min coincubation period with [^{3}H]-RF, ^{125}I-TF, or [^{3}H]-FA at 37 °C. Recycled amounts of [^{3}H]-RF (a), ^{125}I-TF (b), and [^{3}H]-FA (c) after 100 μM (solid black bar), 200 μM (horizontal striped bar), 300 μM (vertical striped bar), and no (open bar) treatment were determined and compared with untreated control cells. These data are expressed as a percentage of control and represent the mean ± SD. Statistical significance was defined by one-way ANOVA with the Newman−Keuls multiple comparison test (*, $p \leq 0.05$; **, $p \leq 0.01$; ***, $p \leq 0.001$).

RF, TF, or FA for use in ligand recycling experiments. Similar to the monensin studies, a concentration-dependent decrease in exocytosis resulted for RF and TF (Figure 4a,c); again, FA (Figure 4b) revealed no change after primaquine treatment. The effect of primaquine on RF exocytosis in MCF-7 cells was more pronounced when compared to that of monensin, suggesting that endosomal acidification and, perhaps, organelle morphology are key factors in RF intracellular processing and proper sorting.

Effect of Altered Cytoskeletal Trafficking of Endosomes. Okadaic acid is a potent inhibitor of protein phosphorylation which may result in the disassembly of cytoskeletal microtubules,[31] among other effects on cellular trafficking. Pretreatment of MCF-7 cells with okadaic acid led to a significant increase in clathrin-dependent exocytosis of RF and TF (Figure 5a, c); however, the retrograde movement of FA of was not significantly affected (Figure 5b). Total exocytosis of RF in untreated cells was approximately 65 pmol/mg protein, which approximately doubled upon okadaic acid treatment, suggesting either an enhanced rate in retrograde movement of recycling vesicles or the missorting of endosomes from other intracellular compartments.

Discussion

In an effort to regulate the cellular homeostasis of numerous endocytosed ligands, polarized epithelial cells intricately control their internalization as well as subsequent subcellular trafficking, metabolism, and exocytic release. Overall, the intracellular trafficking of endosomes is a dynamic process which is largely governed by its intravesicular cargo. For example, transferrin remains attached to its receptor during the entire duration of its intracellular residence and releases iron upon vesicular acidification, followed by receptor and ligand recycling to the plasma membrane for continuous iron sequestration.[11] Alternatively, the intracellular processing of insulin follows multiple paths after dissociation from its receptor, ultimately leading to its

(31) Maples, C. J.; Ruiz, W. G.; Apodaca, G. Both microtubules and Actin filaments are required for efficient postendocytotic traffic of the polymeric immunoglobulin receptor in polarized Madin-Darby canine kidney cells. *J. Biol. Chem.* **1997**, *272*, 6741–6751.

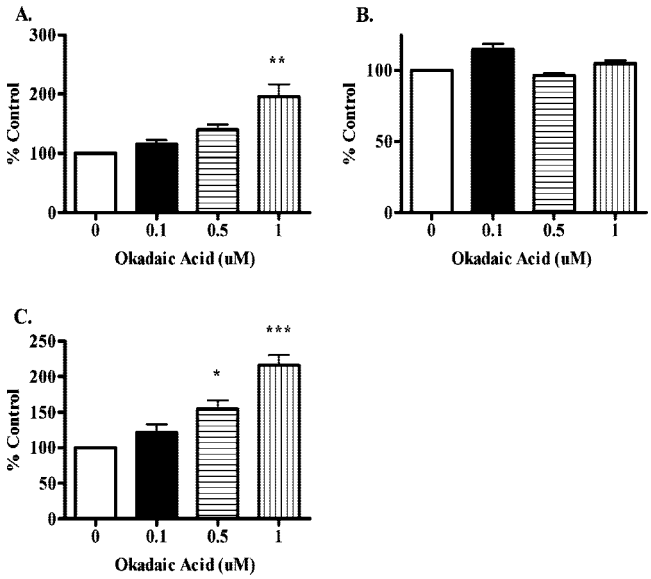

Figure 5. Okadaic acid significantly enhances the exocytosis of RF and TF. MCF-7 cells were preincubated with or without okadaic acid for 30 min, followed by a 20 min coincubation period with [^{3}H]-RF, ^{125}I-TF, or [^{3}H]-FA at 37 °C. Recycled amounts of [^{3}H]-RF (a), ^{125}I-TF (b), and [^{3}H]-FA (c) after 0.1 μM (solid black bar), 0.5 μM (horizontal striped bar), 1 μM (vertical striped bar), and no (open bar) treatment were determined and compared with untreated control cells. These data are expressed as a percentage of control and represent the mean ± SD. Statistical significance was defined by one-way ANOVA with the Newman−Keuls multiple comparison test (*, $p \leq 0.05$; **, $p \leq 0.01$; ***, $p \leq 0.001$).

lysosomal degradation *or* intact recycling.[32] Upon entry into the cytoplasm, early endosomes containing receptor−ligand complexes generally signal H^+ influx to lower vesicular pH, resulting in ligand and receptor dissociation. In the pericentriolar sorting region, tubular structures begin to extend and segregate from the core vesicle while retaining the majority of its membrane proteins. The remaining vesicle retains 70−80% of the original endosome's volume and freely diffusing ligand, which is subsequently committed to its intracellular fate.[16] Thus, the endocytic trafficking of ligands is regulated by a complex set of interdependent intracellular processes. To better comprehend receptor-mediated internalization and trafficking, it is imperative to develop a kinetic model that allows a comprehensive description of the overall endocytic process of each individual ligand−receptor pair. The aim of the present study was to delineate the endocytic components controlling riboflavin regulation.

Our experiments were conducted in human breast cancer cells, MCF-7, which display a relatively high uptake capacity for RF, thereby enabling increased measurement sensitivity

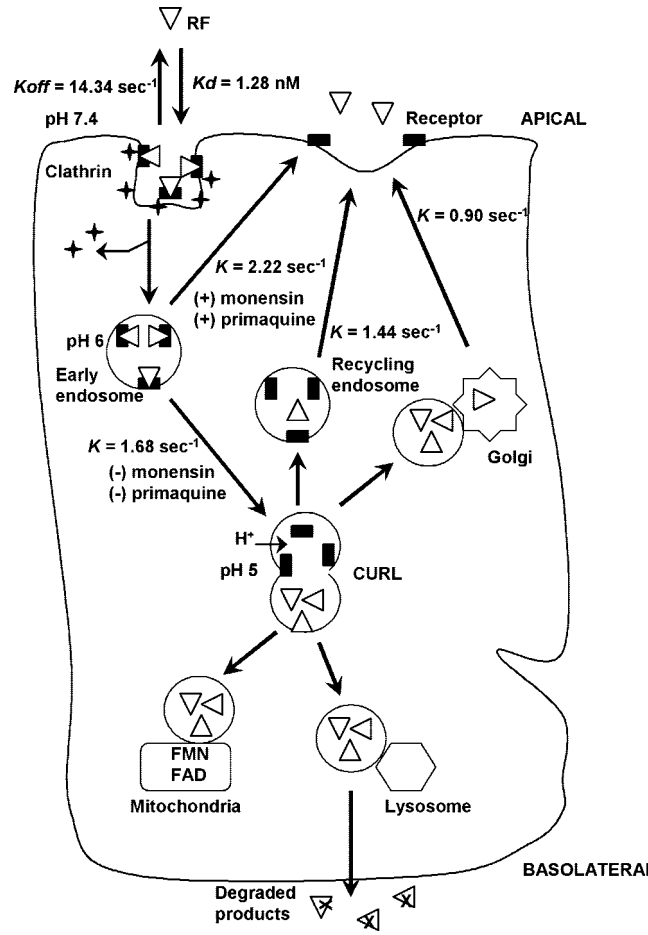

Figure 6. Cellular regulation of riboflavin in MCF-7 cells. RF cell−surface receptor binding is a high affinity association interaction ($k_d = 1.28$ nM) at temperatures ≥ 4 °C which is reversible ($k_{off} = 14.34$ s^{-1}). Receptor binding initiates signaling cascades that lead to receptor−ligand localization into clathrin-coated invaginations in the cellular membrane. At temperatures above 4 °C, the RF−receptor complex is contained within a membrane bound vesicle which is released, with the aid of the scission protein dynamin, to release the endocytic vesicle into the cytosol.[40] Following internalization, RF is contained in an early endosome prior to compartmental sorting, which can lead to its rapid return to the cell surface ($k = 2.22$ s^{-1}). Alternatively, RF-containing early endosomes may continue through a maturation process, where vacuolar proton pumps will be recruited in order to increase the intravesicular H^+ concentration and lower the endosomal pH to 5−6. Following slight acidification, RF traffics through the compartment of uncoupling the receptor from the ligand (CURL) ($k = 1.68$ s^{-1}), where it may become segregated from its receptor. Here, RF may be retained in a recycling endosome for its return to the cell surface ($k = 1.44$ s^{-1}) or sorted to organelle systems for its sorting through the golgi apparatus, utilization in the mitochondrial respiratory chain, or degradation within lysosomes.[9]

while investigating the therapeutic potential of RF in breast cancer tissue. We initially investigated the kinetic profile of RF internalization in this cell line using mathematical models

(32) Marshall, S. Dual pathways for the intracellular processing of insulin. Relationship between retroendocytosis of intact hormone and the recycling of insulin receptors. *J. Biol. Chem.* **1985**, *260*, 13524–13531.

to discern between active internalization alone (eq 2) or in combination with a passive component (eq 3). We demonstrate that the data correspond to a mixed kinetic model while displaying a high affinity/low capacity saturable mechanism at physiological RF concentrations (<12 nM) and a concentration-dependent, linear profile at RF concentrations above basal levels (Figure 1). This is consistent with an overall analysis of the literature describing similar kinetic profiles for ligand uptake governed by receptor-mediated systems.[33]

The next step in our kinetic analysis of the factors governing RF trafficking focused on its exocytosis using a "low-cis" experiment.[24] The premise of this experiment was to record the active externalization of a receptor-mediated ligand, by following the release of preloaded ligand against an increasing extracellular concentration gradient. We reveal that the rate of RF exocytosis accelerated with increasing extracellular RF concentrations; however, the extent of release remained relatively unaffected (Table 1). In comparison, TF, a well-characterized RME ligand known to undergo exocytosis, illustrated equivalent results.[34] These data suggest that RF recycling is an active process linked to the extracellular RF supply, suggesting a compensatory mechanism under periods of RF deficiency.

To study the effects of lysosomal localization on the subsequent sorting or recycling of endocytic ligands, we recorded RF exocytosis at lowered temperatures. It has been well documented that incubation at 4 °C prevents active transport mechanisms, including endo- and exocytosis, which inhibit ligand internalization and may lead to the rapid return of intracellular vesicles to the cell surface,[7] as observed previously for TF.[35] At temperatures below 20 °C, attenuation of vesicle trafficking to lysosomes and other endocytic compartments occurs, resulting in the pericentriolar accumulation of vesicles containing endocytosed ligand.[26,27] In turn, this accumulation prevents continuous ligand internalization and minimizes exocytosis.[13] At 16 °C, we observed a significant decrease in cellular RF and TF release (Figure 2b) compared to that at 37 °C (Figure 2c), suggesting an intracellular buildup of ligand-containing endosomes resulting from the disregulation of vesicular trafficking. For TF, these data are in good agreement with the results published by Nunez and Tapia.[34] Interestingly, TF exocytosis at 4 °C, although significantly less than that at 37 °C, was double the amount released at 16 °C, which has previously been attributed to a putative temperature-dependent decrease in TF−receptor binding affinity leading to the rapid release of apotransferrin.[35] FA exocytosis was not affected by temperature. At 4 °C, RF release was negligible (Figure 2a), and is likely governed by a passive, equilibrative process.

Similar to many endocytosed ligands, RF binds its receptor with high affinity at or near physiological pH, whereas an acidic extracellular milieu results in ligand−receptor dissociation.[6] Accordingly, upon internalization, ligands generally detach from their receptor after vesicular acidification.[30] Thus, treatment with lysomotropic agents, such as monensin and primaquine, results in compartmental neutralization, which can prevent dissociation and segregation of ligands and receptors, and may inhibit tubulovesicular sorting from the recycling endosome,[28] as illustrated previously for insulin.[36] Cells incubated with monensin or primaquine exhibited a significant decrease in apically released RF (Figures 3a and 4a). This indicates that RF efflux is effectively reliant upon the dissociation and endosomal segregation of the RF−receptor complex that, if modified, may result in missorting and/or inefficient cellular processing. Interestingly, RF recycling was more severely affected by primaquine (Figure 4), potentially due to its effect on additional intracellular events mechanistically unrelated to monensin-induced changes. Primaquine has been shown to be a potential antagonist for calmodulin,[27] which has been implicated in intracellular transport of vesicles toward the plasma membrane and is thought to play a role in vesicle recycling.[30,37] In further support of the potential role of calmodulin in RF endocytic transport, we have previously shown a concentration-dependent decrease in RF uptake following treatment with calmodulin antagonists.[7] However, the exact role of calmodulin on RF internalization, trafficking, and recycling warrants further studies.

Studies investigating the role of microtubule-dependent vesicular−ligand recycling have exhibited differential effects, which are cell type dependent, following an indirect okadaic acid effect on microtubule disassembly leading to increases in endocytic trafficking[38] and ligand exocytosis.[9] An earlier study in our laboratory identified possible microtubular regulation of RF internalization and trafficking following functional and structural characterization resulting from okadaic acid treatment.[39] Microtubules form intracellular cytoskeletal networks which serve as a scaffold for bidirec-

(33) Tomei, S.; Yuasa, H.; Inoue, K.; Watanabe, J. Transport functions of riboflavin carriers in the rat small intestine and colon: site difference and effects of tricyclic-type drugs. *Drug Delivery* **2001**, *8*, 119–124.

(34) Nunez, M. T.; Tapia, V. Transferrin stimulates iron absorption, exocytosis, and secretion in cultured intestinal cells. *Am. J. Physiol.* **1999**, *276*, C1085–C1090.

(35) Nishisato, T.; Aisen, P. Uptake of transferrin by rat peritoneal macrophages. *Br. J. Haematol.* **1982**, *52*, 631–640.

(36) Huecksteadt, T.; Olefsky, J. M.; Brandenberg, D.; Heidenreich, K. A. Recycling of photoaffinity-labeled insulin receptors in rat adipocytes. Dissociation of insulin-receptor complexes is not required for receptor recycling. *J. Biol. Chem.* **1986**, *261*, 8655–8659.

(37) Stein, B. S.; Bensch, K. G.; Sussman, H. H. Complete inhibition of transferrin recycling by monensin in K562 cells. *J. Biol. Chem.* **1984**, *259*, 14762–14772.

(38) Hultquist, D. E.; Xu, F.; Quandt, K. S.; Shlafer, M.; Mack, C. P.; Till, G. O.; Seekamp, A.; Betz, A. L.; Ennis, S. R. Evidence that NADPH-dependent methemoglobin reductase and administered riboflavin protect tissues from oxidative injury. *Am. J. Hematol.* **1993**, *42*, 13–18.

(39) D'Souza, V. M.; Bareford, L. M.; Ray, A.; Swaan, P. W. Cytoskeletal scaffolds regulate riboflavin endocytosis and recycling in placental trophoblasts. *J. Nutr. Biochem.* **2006**, *17*, 821–829.

tional vesicular movement from the apical pericentriolar region containing both the early endosomal and recycling compartments.[31] Okadaic acid treatment led to an approximately twofold increase in RF and TF exocytosis, whereas no significant effect was observed on retrograde movement of FA (Figure 5). This increase in RF exocytosis may be explained by okadaic acid induced microtubule modification; however, the effects of okadaic acid on other cellular trafficking pathways, including protein phosphorylation, cannot be underestimated, and further studies are warranted to definitively ascertain microtubular regulation of RF trafficking in MCF-7 cells.

Modifications to the cellular environment, such as changes in temperature, compartmental pH, ligand concentration, and cytoskeletal networks, may alter its trafficking pathways, resulting in missorted vesicles or ligand accumulation in endocytic compartments. Data generated in the present studies were used to calculate the rate and extent of RF internalization and subcellular trafficking to apical sorting regions and organelle compartments (Figure 6). Kinetic analysis revealed RF binds to a specific cell surface receptor with high affinity ($k_d = 1.28$ nM) at temperatures ≥ 4 °C, which is a reversible conjugation corresponding with its dissociation ($k_{off} = 14.34\ s^{-1}$). RF−receptor binding initiates signaling cascades that lead to receptor−ligand localization into clathrin-coated invaginations in the cellular membrane. At temperatures above 4 °C, the RF−receptor complex is contained within a membrane bound vesicle which is released, with the aid of the scission protein dynamin, to release the endocytic vesicle into the cytosol.[40] Following internalization, RF is contained in an early endosome prior to compartmental sorting where RF may rapidly return to the cell surface ($k = 2.22\ s^{-1}$) or follow a slower pathway leading to its efflux via a recycling endosome ($k = 1.44\ s^{-1}$). Alternatively, RF-containing vesicles will recruit vacuolar proton pumps to increase the intravesicular H^+ concentration (pH to 5−6). This slight acidification may induce morphological changes in receptor conformation to enable the dissociation and vesicular segregation of ligands and receptors in a pericentriolar sorting region, namely, the compartment of uncoupling the receptor from the ligand (CURL).[14] RF traffics to the compartment of the uncoupling receptor and ligand ($k = 1.68\ s^{-1}$) prior to association with organelle systems, such as its apical sorting from the golgi apparatus ($k = 0.90\ s^{-1}$). The combined data from the experiments in this study were used to generate a cellular kinetic profile for RF internalization and trafficking between individual subcellular sorting compartments under physiological and biochemically altered environments (Figure 6). Some limitations should be noted in this working model: first, the permeation of ligand in and out of vesicles via passive diffusion has not been taken into account (although this should comprise <10% of overall cargo turnover at the concentrations studied); second, the effect on trafficking of enzymatic RF conversion into its coenzyme forms FMN and FAD, an efficient mechanism for capturing and storing riboflavin within the cell generally referred to as "metabolic trapping",[1] has not been determined and may affect its trafficking kinetics. Further studies are necessary to delineate additional components of RF cellular trafficking, turnover, and homeostasis. Overall, mathematical modeling of RF transport has aided in a more accurate understanding of the multiple parameters involved in its passive as well as active internalization. The establishment of a standard transport model for RF, taking into account all hitherto known parameters, would allow for the identification of any components which may be altered in RF-associated disease states. Finally, using data from the present study, as well as earlier work from our laboratory, we have produced a comprehensive scheme illustrating all identified intracellular trafficking pathways for RF following its clathrin-mediated RME (Figure 6).

Conclusion

Understanding the cellular kinetics and mechanisms regulating RF absorption, intracellular trafficking, and recycling is critical in facilitating future studies aimed at utilizing RF for applications in drug delivery. Identifying RF regulatory processes will allow the characterization of intracellular events which can be manipulated in RF-responsive diseased tissue. Known RME ligands such as TF, FA, and carbohydrates are currently being used to target drug complexes to tissues in specific disease states, such as solid tumors.[41] Here, the application of RME ligands as targeting moieties has increased cellular uptake of drug conjugates. An abundance of clinical evidence has proposed a role of RF molecular sensors in breast and liver cancer progression rendering the RF cellular pathway of high interest in targeting these tissue types. Targeting drug delivery vehicles with high affinity ligands, such as RF, would theoretically allow for a more efficient means of therapy. Thus, a detailed understanding of its intracellular processing will aid in the development of novel therapeutic modalities.

Acknowledgment. This study was partly supported by funding from the Susan G. Komen for the Cure Foundation (to P.W.S.).

MP800046M

(40) Foraker, A. B.; Ray, A.; Claro da Silva, T.; Bareford, L. M.; Hillgren, K. M.; Schmittgen, T. D.; Swaan, P. W. Dynamin 2 Regulates Riboflavin Endocytosis in Human Placental Trophoblasts. *Mol. Pharmacol.* **2007**, *72*, 553–562.

(41) Bareford, L. M.; Swaan, P. W. Endocytic mechanisms for targeted drug delivery. *Adv. Drug Delivery Rev.* **2007**, *59*, 748–758.